Research Square

Preprints are preliminary reports that have not undergone peer review.
They should not be considered conclusive, used to inform clinical practice,
or referenced by the media as validated information.

Reversible sulfite derivatization enhances the colorimetric response of anthocyanin-loaded hydrogel beads for shrimp freshness monitoring

Haomiao Liu
China Agricultural University-Sichuan Advanced Agricultural & Industrial Institute
Xin Li
China Agricultural University
Qinnan Liu
China Agricultural University
Lijun Yin
China Agricultural University-Sichuan Advanced Agricultural & Industrial Institute
Xin Jia
xinjia@cau.edu.cn

China Agricultural University-Sichuan Advanced Agricultural & Industrial Institute

Research Article

Keywords: Anthocyanin sulfite derivative, pH-responsive hydrogel beads, reversible color switching, ammonia response, shrimp freshness monitoring

Posted Date: September 7th, 2026

DOI: https://doi.org/10.21203/rs.3.rs-10488110/v1

License: This work is licensed under a Creative Commons Attribution 4.0 International License.
Read Full License

Additional Declarations: No competing interests reported.

Reversible sulfite derivatization enhances the colorimetric response of anthocyanin-loaded hydrogel beads for shrimp freshness monitoring

Haomiao Liu [a,b,c], Xin Li [b,c], Qinnan Liu [b,c], Lijun Yin [a,b,c], Xin Jia [a,b,c*]

a China Agricultural University-Sichuan Advanced Agricultural & Industrial Institute, Sichuan 610000, China

b Beijing Key Laboratory of Functional Food from Plant Resources, College of Food Science and Nutritional Engineering, China Agricultural University, Beijing 100083, China

c Center of Food Colloids and Delivery for Functionality, College of Food Science and Nutritional Engineering, China Agricultural University, Beijing 100083, China

*Corresponding author: Xin Jia, China Agricultural University-Sichuan Advanced Agricultural & Industrial Institute, Sichuan 610000, China, E-mail: xinjia@cau.edu.cn

Abstract

Anthocyanin-based freshness indicators have attracted considerable attention owing to their natural origin and pH responsiveness; however, their gradual color transition and limited visual contrast often restrict rapid spoilage identification. Although various stabilization strategies have been proposed, few studies have attempted to improve indicator performance through reversible molecular switching of anthocyanins. In this study, a reversible anthocyanin sulfite derivative (ASD) was developed and subsequently immobilized in a pectin–alginate hydrogel to construct a highly responsive colorimetric freshness indicator. The molecular characteristics, pH-responsive behavior, ammonia sensing performance, and shrimp freshness monitoring capability of the indicator were systematically evaluated. ASD exhibited a unique "colored–colorless–colored" transition within the pH range of 1–12, providing a distinct sensing window near neutral conditions. Compared with native anthocyanins, ASD-loaded hydrogel beads showed a 44.1% shorter response time toward ammonia vapor together with a higher final color difference. During refrigerated shrimp storage, the indicator provided earlier visual warning and exhibited strong positive correlations with shrimp pH and total viable count. This study demonstrates that reversible sulfite derivatization provides a feasible molecular switching strategy for improving anthocyanin-based freshness indicators and offers a promising approach for intelligent food packaging applications.

Keywords: Anthocyanin sulfite derivative; pH-responsive hydrogel beads; reversible color switching; ammonia response; shrimp freshness monitoring

1. Introduction

Anthocyanin-based colorimetric indicators provide a simple and intuitive means of monitoring food freshness by converting spoilage-associated chemical changes into visible color signals. They are particularly suitable for protein-rich foods, such as seafood, in which microbial and enzymatic degradation produces ammonia, trimethylamine, and other volatile basic compounds that progressively alter the package headspace (Mohammadalinejhad et al., 2024; Mohseni-Shahri and Moeinpour, 2023). Anthocyanins are widely employed as sensing pigments because of their natural origin, biodegradability, and pronounced pH-dependent structural transformations among flavylium cations, carbinol pseudobases, quinoidal bases, and chalcones (Liu et al., 2022; Luo et al., 2022). Accordingly, anthocyanins have been incorporated into films, hydrogels, fibers, and labels for the visual monitoring of seafood freshness.

However, the practical performance of native anthocyanin indicators is constrained not only by pigment instability but also by their intrinsic color-transition pathway. Their responses commonly extend over a broad pH range and proceed through gradual, overlapping color changes, resulting in poor visual discrimination between adjacent freshness stages (Almasi et al., 2022; Zheng et al., 2022). In particular, the weakly colored hydrated species formed near mildly acidic or neutral conditions may reduce the initial color contrast and delay recognition of early spoilage. Previous studies have mainly improved anthocyanin retention through encapsulation, copigmentation, or polymer interactions (Feitosa et al., 2025). Although these approaches can enhance storage stability, they do not fundamentally reshape the reversible molecular equilibrium responsible for color development. Therefore, engineering the pigment response itself, rather than relying solely on carrier-based stabilization, may provide a more direct route to faster and more distinguishable freshness indication.

Reversible bisulfite addition offers a potential molecular-switching strategy. Bisulfite can nucleophilically attack the C-4 position of the anthocyanin flavylium cation, interrupting the conjugated chromophore and producing a nearly colorless sulfonate adduct; changes in the acid–base environment can subsequently shift this equilibrium and restore colored anthocyanin species (Berké et al., 1998; Brouillard and Elhagechahine, 1980; Jurd, 1964). This reversible bleaching chemistry has long been recognized in wine and pigment systems, but it has rarely been exploited to regulate the response kinetics and visual contrast of intelligent freshness indicators. It remains

unclear whether a bisulfite-derived anthocyanin switch can retain its reversibility after immobilization and whether the resulting molecular response can be translated into an earlier warning of food spoilage (Mercanti et al., 2024; Noël et al., 2026).

To convert this molecular switching behavior into a practical indicator, an appropriate carrier should retain the derivative while permitting rapid mass transfer between the hydrated sensing phase and volatile bases in the package headspace. Calcium-crosslinked alginate provides a water-rich, permeable network, whereas low-methoxyl pectin can participate in additional ionic junctions and interactions with anthocyanin-derived compounds (Chan et al., 2017; Einhorn-Stoll, 2018; Reichembach and de Oliveira Petkowicz, 2021). A pectin–alginate hydrogel may therefore serve as a suitable immobilization matrix. Nevertheless, the carrier should function as a support for the molecular switch rather than obscure its contribution; direct comparison with native anthocyanins under identical matrix and exposure conditions is essential to distinguish the effect of sulfite derivatization from that of encapsulation.

In this study, a reversible anthocyanin sulfite derivative (ASD) was constructed and immobilized in pectin–alginate hydrogel beads for shrimp freshness monitoring. The formation and pH-dependent reversibility of ASD were first characterized, followed by optimization of the hydrogel formulation. The color-response amplitude and kinetics of ASD-loaded beads were then compared directly with those of native-anthocyanin beads during ammonia exposure, and their practical performance was evaluated using shrimp pH and total viable count during refrigerated storage. This work aimed to clarify whether reversible sulfite derivatization can convert anthocyanin structural switching into a faster and more readily interpretable freshness signal, thereby providing a molecular-level strategy for improving anthocyanin-based intelligent packaging.

2. Materials and methods

2.1 Materials

Blueberry anthocyanin extract (25% anthocyanins) was purchased from Lingonberry Cold Region Biotechnology (Daxing'anling, China). Low-methoxyl pectin (degree of esterification: 12%) was obtained from Fangxin Biotechnology (Guangdong, China). Sodium alginate and sodium bisulfite were purchased from Macklin (Shanghai, China) and Aladdin (Shanghai, China), respectively. Fresh shrimp were purchased from a local market in Beijing, China. All other chemicals were of

analytical grade and used without further purification. Deionized water was used throughout the experiments unless otherwise stated.

2.2 Determination of anthocyanin content

The anthocyanin content of the blueberry extract was determined using the pH differential method with slight modifications. Samples were diluted separately with potassium chloride buffer (pH 1.0) and sodium acetate buffer (pH 4.5). Absorbance was measured at 510 and 700 nm using a microplate reader (Thermo Fisher Scientific, USA). The anthocyanin content was calculated using the following equation (1):

$$\text{Anthocyanin content (mg/L)} = \frac{A \times MW \times DF \times 1000}{\varepsilon \times l} \quad (1)$$

where:

$$A = (A_{510} - A_{700})_{pH1.0} - (A_{510} - A_{700})_{pH4.5}$$

In the equation, MW is the molecular weight of cyanidin-3-O-glucoside (449.2 g/mol), DF is the dilution factor, ε is the molar extinction coefficient (26,900 $L \cdot mol^{-1} \cdot cm^{-1}$), and l is the path length (1 cm). Each sample was measured in triplicate, and the results were expressed as milligrams of cyanidin-3-O-glucoside equivalents per liter of sample (mg cyanidin-3-O-glucoside equivalents/L).

2.3 Preparation of anthocyanin sulfite derivatives (ASD)

Anthocyanin sulfite derivatives (ASD) were prepared according to previously reported sulfite-addition procedures with slight modifications (Brouillard and Elhagechahine, 1980; Jurd, 1964). Blueberry anthocyanin extract and sodium bisulfite were separately dissolved in citric acid buffer (pH 3.0). The anthocyanin concentration was fixed at 0.1 g/L, while sodium bisulfite concentrations were adjusted to 0.1–1.0 g/L. The mixtures were stirred at 25 ± 2 °C for 30 min.

2.4 Determination of bleaching degree and color recovery

The bleaching degree of the reaction system was evaluated by measuring the absorbance at 510 nm and calculated according to equation (2). To assess color recovery, the resulting solutions were acidified with pH 1.0 buffer and the absorbance at 510 nm was recorded again, and the recovery efficiency was calculated according to equation (3). The optimal anthocyanin-to-bisulfite ratio was selected based on both bleaching efficiency and color recovery performance.

$$\text{bleaching degree (\%)} = \frac{A_0 - A_{pH3.0}}{A_0} \times 100\% \quad (2)$$

$$\text{color recovery efficiency (\%)} = \frac{A_{pH1.0}}{A_{0'}} \times 100\% \quad (3)$$

where A_0 is the absorbance of the pH 3.0 anthocyanin solution at 510 nm; $A_{0'}$ is the absorbance of the pH 1.0 anthocyanin solution at 510 nm; $A_{pH3.0}$ is the absorbance of the pH 3.0 derivative solution at 510 nm; $A_{pH1.0}$ is the absorbance of the pH 1.0 derivative solution at 510 nm.

2.5 Characterization of ASD

2.5.1 UV–Vis spectroscopy

The UV–Vis spectra of native anthocyanins and ASD were recorded in buffers with pH values ranging from 1.0 to 12.0. Spectral scanning was performed from 350 to 700 nm using a microplate reader. The corresponding color changes were photographed under identical lighting conditions.

2.5.2 pH transition analysis

The pH-responsive behavior of ASD was evaluated by acid–base titration. ASD solution prepared in pH 1.0 buffer was gradually titrated with 0.05 M NaOH while continuously monitoring pH and visual color changes. After the occurrence of a distinct color transition, reverse titration was performed using 0.05 M HCl until the original color was restored. The pH values corresponding to each color transition point were recorded.

2.5.3 FTIR analysis

Native anthocyanins, ASD, and sodium bisulfite were freeze-dried prior to analysis. Samples were mixed with spectroscopic-grade KBr and compressed into transparent pellets. FTIR spectra were collected using a Fourier transform infrared spectrometer over the range of 4000–400 cm^{-1} at a resolution of 4 cm^{-1} with 64 scans.

2.6 Preparation of ASD-loaded hydrogel beads

ASD-loaded hydrogel beads were prepared using an ionic gelation method with slight modifications. Briefly, pectin and sodium alginate were separately dispersed in deionized water to obtain 3.75% (w/v) stock solutions and stirred overnight at room temperature to ensure complete hydration. The pectin solution, sodium alginate solution, and ASD solution were then mixed at predetermined ratios and stirred for at least 30 min to obtain a homogeneous mixture.

Subsequently, 50 mL of the mixed solution was dropped into 100 mL $CaCl_2$ solution under gentle stirring (100 rpm) using a syringe. After crosslinking for 30 min at room temperature, the hydrogel

beads were collected by filtration, washed three times with deionized water to remove excess calcium ions, and stored at 4 °C until further use.

2.7 Optimization of hydrogel bead formulation

2.7.1 Single-factor experiments

Single-factor experiments were conducted to investigate the effects of anthocyanin concentration (0.1–2 g/L), pectin proportion (0–1.0), total polysaccharide concentration (1.0–3.0%), and $CaCl_2$ concentration (1.0–5.0%) on the encapsulation efficiency of hydrogel beads. During each experiment, only one factor was varied while the remaining parameters were kept constant. Encapsulation efficiency was used as the evaluation index.

2.7.2 Response surface optimization

Based on the results of the single-factor experiments, a Box–Behnken design was employed to optimize the formulation of ASD-loaded hydrogel beads. Anthocyanin concentration (A), pectin proportion (B), and total polysaccharide concentration (C) were selected as independent variables, while encapsulation efficiency was used as the response variable. Experimental design, regression analysis, and optimization were performed using Design-Expert software.

2.8 Encapsulation efficiency

The encapsulation efficiency (EE) of hydrogel beads was determined using an indirect method. After gel bead formation, the filtrate was collected and the anthocyanin concentration was quantified according to the method described in Section 2.2. Encapsulation efficiency was calculated from the difference between the total anthocyanin content initially added and the amount remaining in the filtrate, according to equation (4).

$$EE\ (\%)=\frac{M-m}{M}\times 100\% \quad (4)$$

where M is the total anthocyanin content before encapsulation and m is the anthocyanin content detected in the filtrate.

2.9 Colorimetric characterization

Color parameters (L*, a*, and b*) of hydrogel beads were measured using a colorimeter (Konica Minolta, Japan). Total color difference ΔE was calculated according to the CIEDE2000 color difference equation using untreated hydrogel beads as the reference.

2.10 pH responsiveness of hydrogel beads

To evaluate pH responsiveness, 2.0 g of hydrogel beads were immersed in 5 mL buffer solutions with pH values ranging from 1.0 to 12.0 for 2 min. After treatment, color parameters were measured as described in Section 2.9. Hydrogel beads prepared with native anthocyanins were used as controls.

2.11 Ammonia response behavior

The ammonia sensitivity of ASD-loaded and native anthocyanin-loaded hydrogel beads was evaluated using a static headspace exposure system. Briefly, 2.0 g of hydrogel beads and 2 mL of 5% ammonia solution were separately placed in open Petri dishes. The two dishes were then placed together in a larger sealed Petri dish to allow the beads to be exposed to ammonia vapor. The color changes of the hydrogel beads were recorded at predetermined intervals over 30 min.

At each time point, the color parameters (L*, a*, and b*) of the hydrogel beads were measured as described in Section 2.9, and the total color difference ΔE was calculated relative to the initial color state before ammonia exposure. ASD-loaded hydrogel beads were compared with native anthocyanin-loaded hydrogel beads prepared under the same formulation conditions.

To quantitatively compare the ammonia-response rates of the two types of hydrogel beads, the time required to reach 95% of the final color response (t_{95}) was determined from the ΔE-time curves. The final color response, denoted as ΔE, was defined as the stable ΔE value measured at the end of ammonia exposure. The relative color response at time (t) was calculated according to equation (5):

$$R_t(\%)=\frac{\Delta E_t}{\Delta E_{30}}\times 100 \tag{5}$$

where R_t is the relative color response at time (t), ΔE_t is the total color difference at time (t), and ΔE_{30} is the final stable total color difference.

The t_{95} value was defined as the time required for the hydrogel beads to reach 95% of ΔE_{30}. When the 95% response threshold fell between two adjacent experimental time points, t_{95} was estimated by linear interpolation according to equation (6):

$$t_{95}=t_1+\frac{0.95\Delta E_{30}-\Delta E_{t_1}}{\Delta E_{t_2}-\Delta E_{t_1}}(t_2-t_1) \tag{6}$$

where t_1 and t_2 are the two adjacent time points before and after the 95% response threshold,

212 respectively.

213 2.12 Shrimp freshness monitoring

214 2.12.1 Freshness monitoring experiment

215 To evaluate the applicability of the developed indicator in real food systems, hydrogel beads
216 prepared from ASD and native anthocyanins were used for monitoring shrimp freshness during
217 refrigerated storage. Prior to gel bead preparation, the pH values of ASD and anthocyanin
218 solutions were adjusted to 3, 4, 5, 6, and 7, respectively, resulting in ten different types of hydrogel
219 beads.

220 Two fresh shrimp (23.41 ± 0.73 g) and a Petri dish containing hydrogel beads were placed
221 together in a sterilized transparent plastic container and stored at 4 °C for 8 days. Samples were
222 collected at predetermined intervals for the determination of shrimp quality parameters and color
223 changes of the hydrogel beads.

224 2.12.2 pH determination

225 The pH value of shrimp samples was determined according to GB 5009.237-2016 with slight
226 modifications. Briefly, 5 g of shrimp muscle was homogenized with 45 mL of boiled and cooled
227 deionized water and allowed to stand for 30 min at room temperature. The mixture was then
228 centrifuged at 11,000 rpm for 12 min at 4 °C, and the pH of the supernatant was measured using a
229 calibrated pH meter.

230 2.12.3 Total viable count (TVC)

231 The total viable count (TVC) was determined according to GB 4789.2-2022. Briefly, 5 g of shrimp
232 muscle was homogenized with 45 mL sterile saline solution (0.85%, w/v). Serial decimal dilutions
233 were prepared and plated on plate count agar. After incubation at 30 °C for 72 h, colonies were
234 counted and expressed as lg(CFU/g).

235 2.13 Statistical analysis

236 All experiments were performed in triplicate unless otherwise stated. Results are presented as
237 mean ± standard deviation (SD). Statistical analyses were performed using SPSS 27.0 (IBM Corp.,
238 Armonk, NY, USA). Significant differences among treatments were evaluated by one-way
239 analysis of variance (ANOVA) followed by Duncan's multiple range test at a significance level of
240 $p < 0.05$. Graphs were plotted using Origin 2025 software.

241 3. Results and discussion

3.1 Construction and reversible pH-responsive behavior of anthocyanin sulfite derivatives

3.1.1 Optimization of the anthocyanin–bisulfite reaction conditions

Increasing sodium bisulfite from 0.1 to 1.0 g/L increased bleaching from 60.23% to 79.21%, but reduced color recovery from 97.59% to 52.81% (Fig. 1). The plateau in bleaching above 0.6 g/L and the concurrent loss of recovery show that excess bisulfite favored persistence of the adduct rather than useful reversibility. A concentration of 0.3 g/L (anthocyanin-to-bisulfite mass ratio 1:3) was therefore selected, providing 71.29% bleaching degree and 86.50% recovery. This compromise established a low-background state while retaining the capacity for signal regeneration.

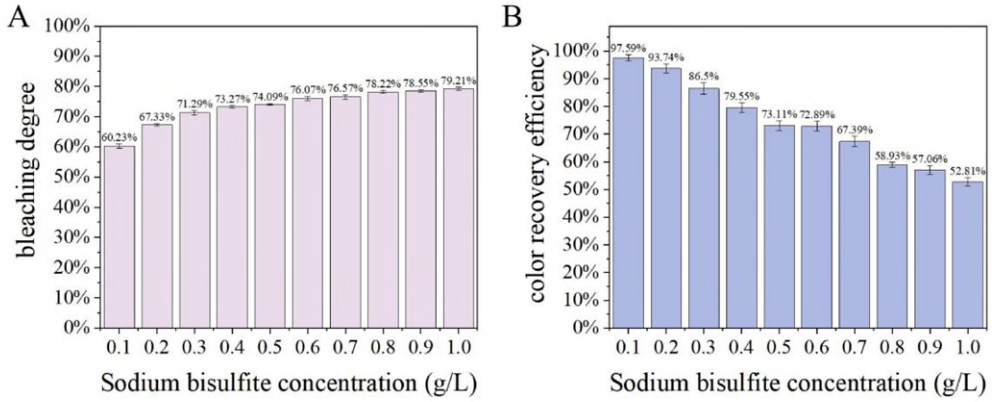


Fig. 1. Effect of sodium bisulfite concentration on the (A) bleaching degree and (B) color recovery efficiency of anthocyanins. Anthocyanin concentration was fixed at 0.1 g/L.

3.1.2 pH-dependent chromatic behavior and UV–Vis spectral characterization of ASD

Native anthocyanins showed the expected progressive spectral changes from the red flavylium form at pH 1–3 toward hydrated, quinoidal, and chalcone-related forms as pH increased (Fig. 2A). ASD instead retained a strong band near 510 nm at pH 1, showed markedly reduced visible absorption from pH 2 to 7, and regained visible absorption near pH 8 (Fig. 2B–C). Bidirectional titration located transitions at pH 1.65–1.71, 2.78–2.85, and 7.42–7.46, with closely matched forward and reverse values. Thus, derivatization replaced a broad gradual response with a reproducible switching interval that brackets the neutral-to-alkaline conditions relevant to volatile-base detection (Brouillard and Elhagechahine, 1980; Timberlake and Bridle, 1967).

Unlike conventional stabilization, which mainly preserves the native pigment, bisulfite addition created a reversible low-color state and redefined how the visible signal was generated. This

molecular-level reshaping directly addressed the overlapping transitions and weak stage-to-stage discrimination of native anthocyanins, providing a low background below the trigger region and stronger optical separation after chromophore regeneration.

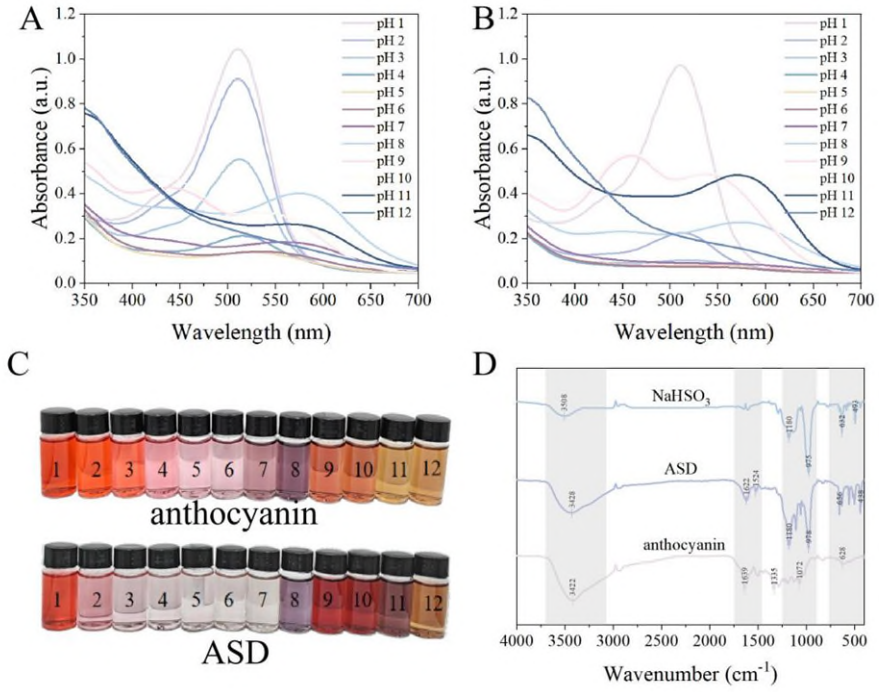


Fig. 2. pH-dependent spectral and colorimetric properties of native anthocyanins and anthocyanin sulfite derivatives (ASD). (A) UV–Vis spectra of anthocyanins at pH 1–12. (B) UV–Vis spectra of ASD at pH 1–12. (C) Representative photographs of anthocyanins and ASD at different pH values. (D) FTIR spectra of anthocyanins, ASD, and sodium bisulfite.

Table 1. Transition pH values of ASD during forward and reverse acid–base titration.

Color transition	pH range	Forward titration (NaOH)	Reverse titration (HCl)
Red → Pink	1–2	1.65 ± 0.05	1.71 ± 0.06
Pink → Colorless	2–3	2.78 ± 0.09	2.85 ± 0.11
Colorless → Purple	7–8	7.46 ± 0.13	7.42 ± 0.21

3.1.3 FTIR characterization of ASD

FTIR spectra showed a shift in the broad O–H region from approximately 3424 to 3432 cm^{-1} and an additional feature near 1176 cm^{-1} assigned to S=O stretching (Fig. 2D). Together with the UV–Vis response and reversible titration, these changes support anthocyanin–bisulfite interaction and formation of an ASD adduct. The assignment is consistent with the reported sulfonate-related

vibration of anthocyanin–bisulfite adducts, but FTIR alone cannot establish the C-4 addition structure; the original structural studies used complementary chemical and spectroscopic evidence (Berké et al., 1998; Brouillard and Elhagechahine, 1980).

3.2 Optimization of ASD-loaded pectin–alginate hydrogel beads

3.2.1 Effects of formulation variables on encapsulation efficiency

Single-factor tests identified anthocyanin concentration, pectin proportion, and total polysaccharide concentration as influential variables (Fig. 3). Encapsulation increased up to an anthocyanin concentration of 1.0 g/L and a total polysaccharide concentration of 2.0%, but did not improve at higher levels, consistent with a balance between network retention, viscosity, and pigment diffusion. Pectin-rich formulations retained more pigment than alginate-rich formulations, plausibly because pectin structure regulates Ca^{2+}-induced network organization (Cui et al., 2026). $CaCl_2$ concentration had no significant effect from 1% to 5%; 1% was therefore retained. Similar alginate microbead studies have shown that immobilization changes pigment retention, particle characteristics, and release behavior, emphasizing that carrier composition and network porosity jointly determine the amount of anthocyanin retained (Mohammadalinejhad et al., 2023).

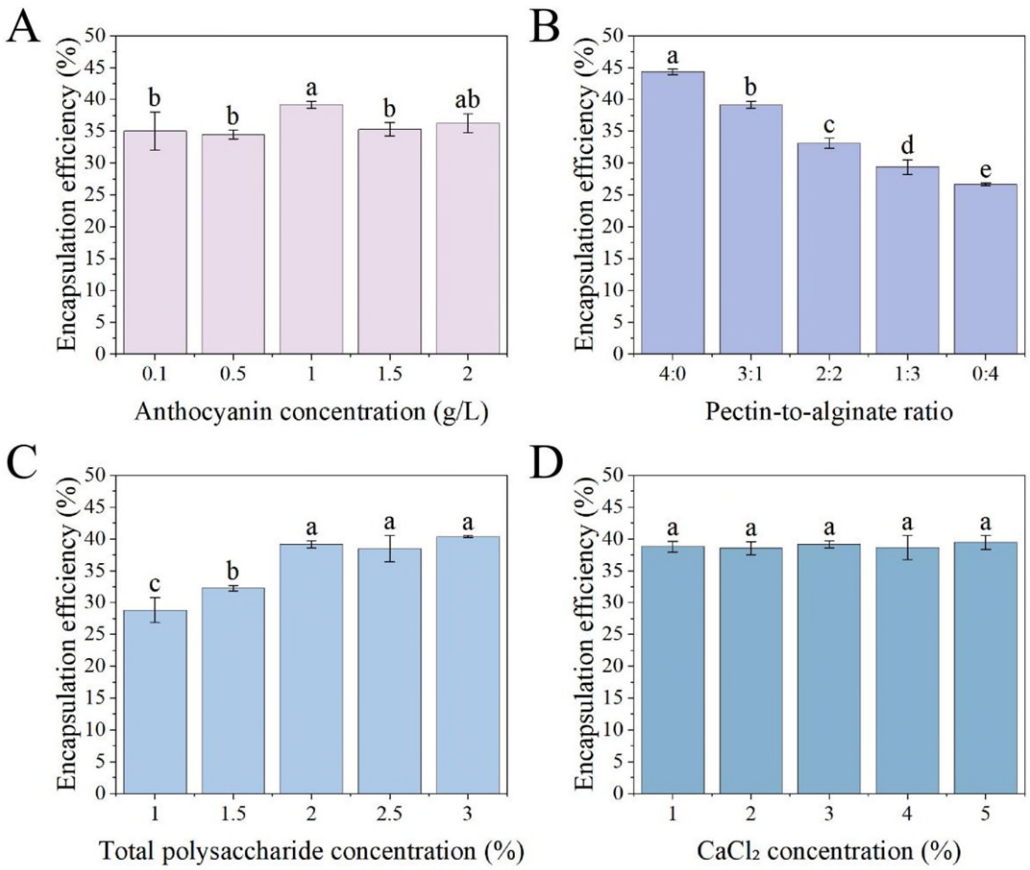


Fig. 3. Effects of formulation variables on the encapsulation efficiency of ASD-loaded hydrogel beads: (A) anthocyanin concentration; (B) pectin-to-alginate ratio; (C) total polysaccharide concentration; and (D) $CaCl_2$ concentration. Different lowercase letters indicate significant differences among treatments ($p < 0.05$).

3.2.2 Response surface optimization and validation of the hydrogel bead formulation

The Box–Behnken model was significant ($p < 0.0001$) with a non-significant lack of fit ($p > 0.05$), $R^2 = 0.9761$, adjusted $R^2 = 0.9454$, predicted $R^2 = 0.7550$, and CV = 1.75% (Tables S1–S3). Anthocyanin concentration and pectin proportion exerted the strongest effects, including a significant interaction, whereas the effect of total polysaccharide concentration was more moderate (Fig. 4). The practical optimum—0.12% anthocyanin, a pectin proportion of 0.825, and 2.6% total polysaccharides—gave 51.48 ± 0.57% encapsulation, close to the predicted 51.18%. The agreement validates the formulation for sensing tests, although encapsulation efficiency alone does not establish long-term bead stability.

Although the model described the experimental domain well, the lower predicted R^2 relative to the

adjusted R^2 indicates that extrapolation beyond the tested factor ranges should be avoided. The response surfaces also show diminishing gains at high anthocyanin or polymer levels. This behavior is physically plausible: increased pigment supply can improve retained mass, but excessive loading promotes loss to the crosslinking bath, while high polymer concentration raises viscosity and can impair homogeneous droplet formation. The selected formulation should therefore be interpreted as a practical optimum for this preparation method rather than a universal maximum for pectin–alginate systems.

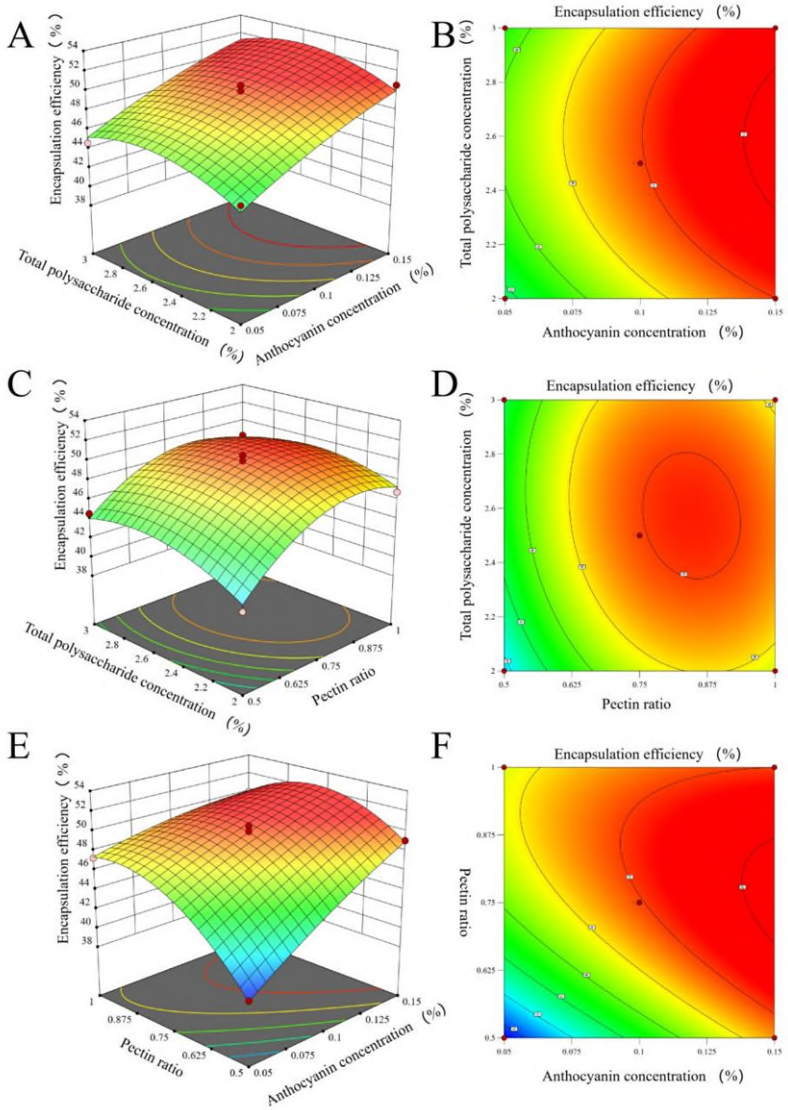


Fig. 4. Response surface plots and contour plots illustrating the interactive effects of formulation variables on the encapsulation efficiency of ASD-loaded hydrogel beads: (A, B) anthocyanin concentration and pectin proportion; (C, D) anthocyanin concentration and total polysaccharide concentration; and (E, F) pectin proportion and total polysaccharide concentration.

3.3 pH-responsive colorimetric performance of ASD-loaded hydrogel beads

ASD-loaded beads showed two principal response regions (Table 2). Relative to untreated beads, ΔE was 6.39 ± 0.39 at pH 1, remained low (1.19–1.55) at pH 2–5, and rose to 5.90 ± 0.06 and 9.30 ± 0.26 at pH 7 and 8, respectively. The maximum at pH 8 confirms that immobilization retained the ASD switching window and positioned the strongest response in the range expected during accumulation of alkaline spoilage volatiles. This quantitative separation, rather than the individual color names, is the key advantage over a gradual anthocyanin response. This retention of a reversible response after gelation agrees with blueberry-extract-loaded alginate hydrogel beads, which also maintained pH-dependent reversibility after immobilization (Viscusi and Gorrasi, 2024). However, the present ASD system differs in producing a deliberately suppressed baseline followed by color recovery, rather than relying only on the native anthocyanin equilibrium. The preserved transition after immobilization indicates that the pectin–alginate network retained the pigment while remaining sufficiently permeable to alkaline species; the carrier therefore translated, rather than created, the molecular switching behavior.

The low ΔE interval at pH 2–5 provides a stable baseline from which the alkaline response can be distinguished, whereas the marked increase between pH 6 and 8 indicates a relatively narrow operational transition. This distribution is more useful than a uniformly changing indicator because small fluctuations during preparation or early storage are less likely to be mistaken for spoilage. The response at pH 1 confirms reversibility under strong acid but is not central to seafood monitoring. For practical interpretation, calibration should therefore focus on the neutral-to-alkaline branch and establish a ΔE threshold corresponding to an independently measured acceptability limit. Matrix-assisted sensitivity enhancement has also been reported through chondroitin-sulfate copigmentation, where ionic association increased the pH and ammonia responsiveness of blueberry-anthocyanin films (Bao et al., 2022). In contrast, ASD modifies the pigment reaction pathway itself, which supports the novelty of molecular switching relative to conventional copigmentation.

Table 2. Color parameters and total color difference of ASD-loaded hydrogel beads exposed to buffer solutions at different pH values.

pH	Color	L*	a*	b*	ΔE

1		41.49 ± 0.13^{g}	11.14 ± 0.64^{a}	6.33 ± 0.21^{a}	6.39 ± 0.39^{bc}
2		44.16 ± 0.06^{ef}	5.03 ± 0.08^{b}	4.06 ± 0.00^{cd}	1.19 ± 0.01^{g}
3		44.23 ± 0.06^{def}	4.45 ± 0.00^{c}	3.92 ± 0.04^{d}	1.55 ± 0.01^{g}
4		44.57 ± 0.06^{de}	4.34 ± 0.01^{c}	4.13 ± 0.10^{bcd}	1.45 ± 0.01^{g}
5		45.35 ± 0.11^{c}	4.35 ± 0.06^{c}	4.37 ± 0.04^{b}	1.32 ± 0.04^{g}
6		43.79 ± 0.16^{f}	3.61 ± 0.05^{d}	4.06 ± 0.16^{cd}	2.53 ± 0.01^{f}
7		46.62 ± 0.17^{b}	2.69 ± 0.01^{e}	-0.75 ± 0.04^{h}	5.90 ± 0.06^{c}
8		50.68 ± 0.28^{a}	1.77 ± 0.11^{f}	-2.22 ± 0.03^{i}	9.30 ± 0.26^{a}
9		41.69 ± 0.25^{g}	5.03 ± 0.21^{b}	4.28 ± 0.16^{bc}	3.23 ± 0.26^{e}
10		38.97 ± 0.11^{h}	2.85 ± 0.06^{e}	3.28 ± 0.05^{e}	6.44 ± 0.12^{b}
11		44.66 ± 0.01^{d}	2.76 ± 0.03^{e}	1.51 ± 0.01^{f}	4.09 ± 0.02^{d}
12		41.75 ± 0.39^{g}	1.83 ± 0.09^{f}	1.13 ± 0.19^{g}	6.05 ± 0.45^{bc}

Values are presented as mean ± SD (n = 3). Different lowercase letters within the same column indicate significant differences among treatments ($p < 0.05$). ΔE values were calculated relative to the untreated beads.

3.4 Ammonia sensing performance of ASD-loaded hydrogel beads

Ammonia exposure revealed both a larger signal and faster kinetics for ASD-loaded beads (Fig. 5). Their ΔE approached 5.7–5.8, compared with 4.1–4.2 for native-anthocyanin beads, and the t_{95} decreased from 12.22 to 6.83 min—a 44.1% reduction. Changes in L*, a*, and b* were consistent with this rapid development but did not alter the kinetic conclusion. Ammonia dissolves in the aqueous bead phase and raises local pH, promoting ASD dissociation and chromophore regeneration. Native anthocyanins instead redistribute gradually among multiple equilibrium forms. The improvement therefore reflects a more efficient signal-generation pathway, not merely a different final hue. Previous shrimp indicators based on copigmented starch films or gelatin/agar composites likewise produced visually recognizable responses to volatile bases, but their performance was mainly evaluated through color trajectories and freshness correlations rather than a normalized kinetic endpoint (Bao et al., 2022; Kim et al., 2022). The present t_{95} analysis therefore adds a direct measure of warning speed under matched carrier conditions.

The ΔE–time profiles further distinguish response rate from end-point contrast. ASD beads

accumulated most of their signal during the first few minutes, whereas native-anthocyanin beads approached their lower plateau more gradually. Reporting t_{95} relative to each material's own 30-min response reduces the influence of different final amplitudes and permits a kinetic comparison. Nevertheless, the static 5% ammonia system represents an accelerated challenge rather than a package-realistic concentration. Future work should determine detection limits and fit concentration-dependent kinetic models using ammonia and trimethylamine levels representative of seafood headspaces. This limitation is important because reported alginate-bead systems have quantified NH_3 and trimethylamine detection limits, illustrating the concentration-dependent validation still required before comparing sensor sensitivity across studies (Viscusi and Gorrasi, 2024).

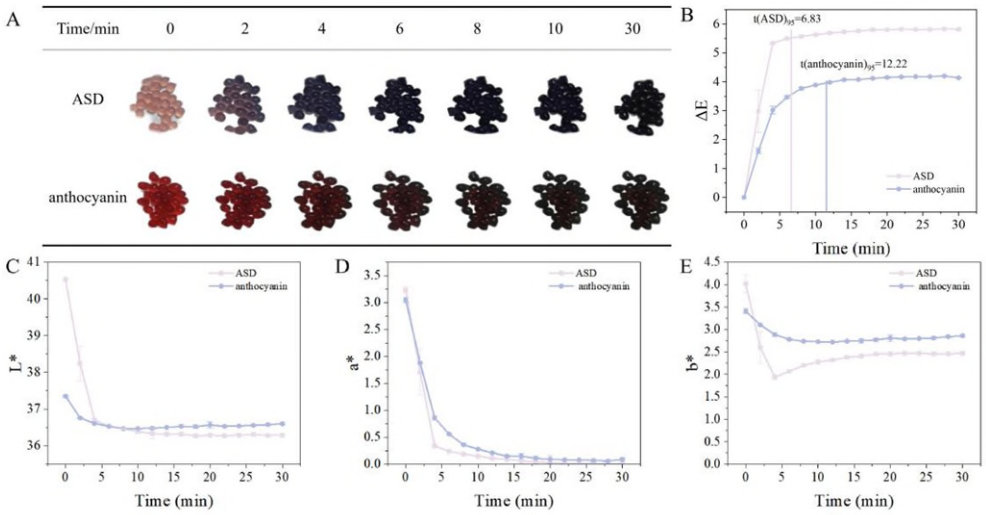


Fig. 5. Time-dependent colorimetric responses of ASD-loaded and native anthocyanin-loaded hydrogel beads exposed to ammonia vapor. (A) Representative photographs during ammonia exposure. (B) Changes in total color difference (ΔE) and the time required to reach 95% of the final response (t_{95}). (C–E) Changes in L*, a*, and b*, respectively. ΔE values were calculated relative to the initial state at 0 min.

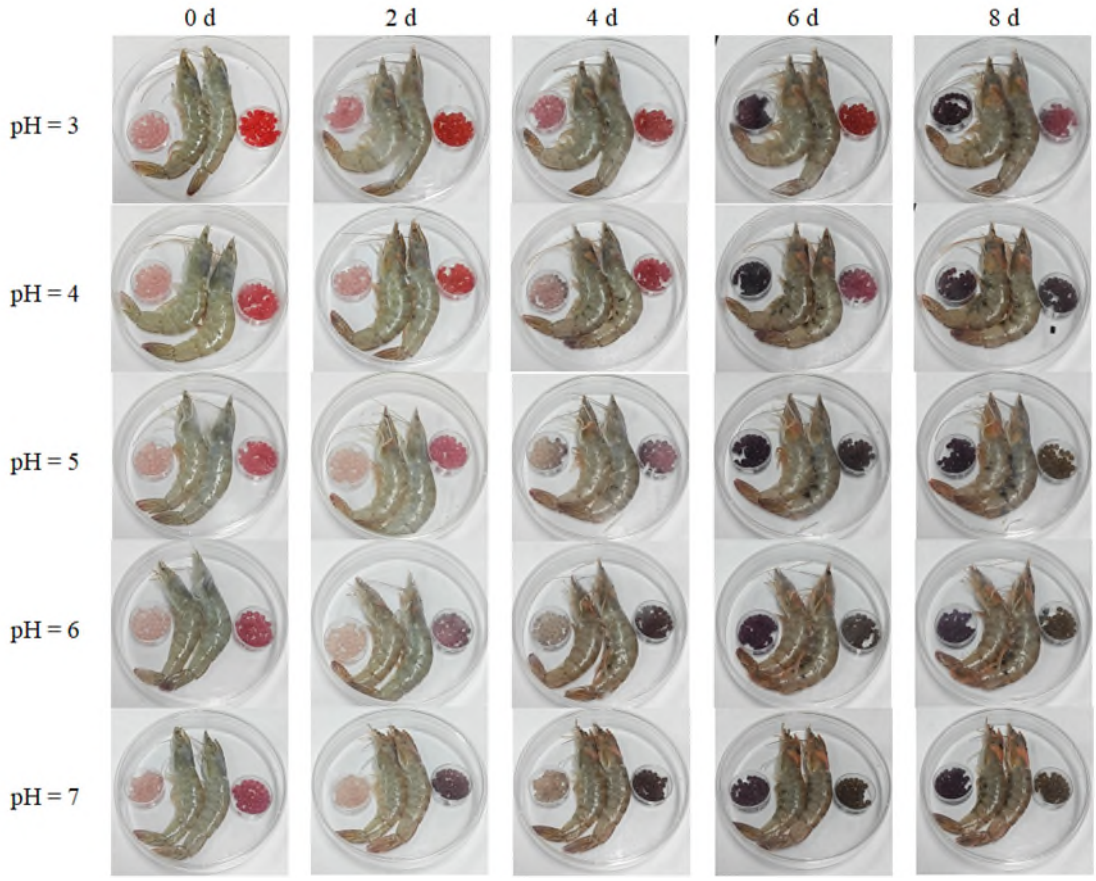
3.5 Application of ASD-loaded hydrogel beads for shrimp freshness monitoring

3.5.1 Visual color changes and freshness evolution during shrimp storage

Over 8 d of storage at 4 °C, shrimp TVC increased from 3.55 to 6.09 lg(CFU/g) and pH from 7.17 to 7.92 (Table 3), consistent with microbial growth and accumulation of alkaline metabolites. ASD-loaded beads responded earlier than corresponding native-anthocyanin beads; at initial pH 4,

ΔE increased from 0 on day 0 to 4.38 on day 4 and 5.85 on day 6, whereas the native control showed a lower response over the first 6 d. This earlier quantitative warning coincided with TVC exceeding 5.0 lg(CFU/g) on day 4 and approaching the commonly used 6.0 lg(CFU/g) acceptability threshold by day 8 (Kaewprachu et al., 2024). According to the TVC-based classification adopted by Yan et al., (2022), this value corresponded to second-grade freshness, indicating that the marked response of the ASD-loaded beads occurred at the onset of freshness loss.A comparable alginate-hydrogel-bead study found strong correlations ($r \geq 0.8$) between indicator color and multiple shrimp deterioration indices, including viable counts, pH, TVB-N, and biogenic amines (Mohammadalinejhad et al., 2024). The present results are directionally consistent, although the absence of TVB-N and amine measurements limits direct chemical validation of the volatile-base mechanism in the food trial.

The day-4 response is particularly relevant because it appeared during the transition from initially low microbial counts toward advanced deterioration, rather than only after the final sampling point. The slight non-monotonicity of ΔE between days 6 and 8 also shows that an indicator should not be evaluated solely by expecting continuous numerical growth. Changes in the proportions of ammonia, amines, carbon dioxide, and water vapor can alter anthocyanin equilibria and optical properties. A practical label would therefore require predefined response categories or image-based calibration supported by larger storage trials, rather than direct interpolation from a single ΔE trajectory. Non-monotonic or matrix-dependent color behavior has also been observed in shrimp-monitoring films, supporting the use of multivariate calibration rather than a single terminal photograph (Kaewprachu et al., 2024).



408

409 Fig. 6. Visual color changes of ASD-loaded and native anthocyanin-loaded hydrogel beads during

410 shrimp storage at 4 °C.

411 Table 3. Changes in shrimp pH, TVC, and ΔE values of hydrogel beads during storage at 4 °C.

	Time/d	0	2	4	6	8
	pH	7.17 ± 0.03^{c}	7.36 ± 0.17^{bc}	7.15 ± 0.17^{c}	7.61 ± 0.28^{ab}	7.92 ± 0.27^{a}
	TVC/ lg(CFU/g)	3.55 ± 0.04^{d}	3.64 ± 0.11^{d}	5.01 ± 0.16^{c}	5.58 ± 0.08^{b}	6.09 ± 0.17^{a}
ASD ΔE	pH=3	0.00^{e}	1.54 ± 0.17^{d}	2.36 ± 0.17^{c}	6.77 ± 0.09^{a}	6.34 ± 0.29^{b}
	pH=4	0.00^{e}	0.76 ± 0.10^{d}	4.38 ± 0.58^{c}	5.85 ± 0.07^{a}	5.34 ± 0.16^{b}
	pH=5	0.00^{d}	0.93 ± 0.16^{c}	4.86 ± 0.13^{b}	6.10 ± 0.14^{a}	5.89 ± 0.09^{a}
	pH=6	0.00^{d}	1.14 ± 0.20^{c}	3.48 ± 0.51^{b}	5.45 ± 0.04^{a}	5.50 ± 0.17^{a}
	pH=7	0.00^{d}	0.77 ± 0.16^{c}	2.41 ± 0.05^{b}	4.83 ± 0.17^{a}	4.93 ± 0.11^{a}
Anthocyanin ΔE	pH=3	0.00^{d}	1.28 ± 0.28^{c}	2.45 ± 0.01^{b}	2.43 ± 0.35^{b}	4.19 ± 0.10^{a}
	pH=4	0.00^{e}	0.94 ± 0.25^{d}	1.76 ± 0.19^{c}	3.97 ± 0.19^{b}	5.48 ± 0.07^{a}
	pH=5	0.00^{e}	1.54 ± 0.13^{d}	4.90 ± 0.07^{c}	6.78 ± 0.10^{a}	6.45 ± 0.15^{b}
	pH=6	0.00^{d}	3.39 ± 0.22^{c}	4.59 ± 0.12^{ab}	4.71 ± 0.09^{a}	4.42 ± 0.01^{b}

	pH=7	0.00^{d}	3.59 ± 0.17^{c}	4.17 ± 0.02^{a}	4.09 ± 0.09^{a}	3.88 ± 0.09^{b}

Values are presented as mean ± SD (n = 3). Different lowercase letters within the same row indicate significant differences among storage times ($p < 0.05$). ΔE values were calculated relative to the corresponding beads on day 0.

Pearson analysis showed positive associations between ΔE of all ASD formulations and TVC, together with generally positive associations with shrimp pH (Fig. 7A). Native-anthocyanin formulations were less consistent, including a negative association between ACN-7 and shrimp pH (Fig. 7B). Considering response timing and correlation patterns, ASD beads prepared at pH 4 provided the best balance between baseline stability and early response, translating the engineered switching window into a more readily interpretable signal as microbial deterioration became substantial. These results indicate that sulfite derivatization improved not only ammonia-response speed but also the consistency with which bead color difference tracked real-food deterioration. Initial bead pH nevertheless remains a critical design variable. Similar agreement between anthocyanin-indicator color and shrimp pH, TVC, or TVB-N has been reported for copigmented starch films, gelatin/agar films, CMC films, and alginate beads (Bao et al., 2022; Kaewprachu et al., 2024; Kim et al., 2022; Mohammadalinejhad et al., 2024). Relative to those systems, the main contribution here is not simply successful freshness tracking, but the matched demonstration that reversible sulfite derivatization accelerates the color response.

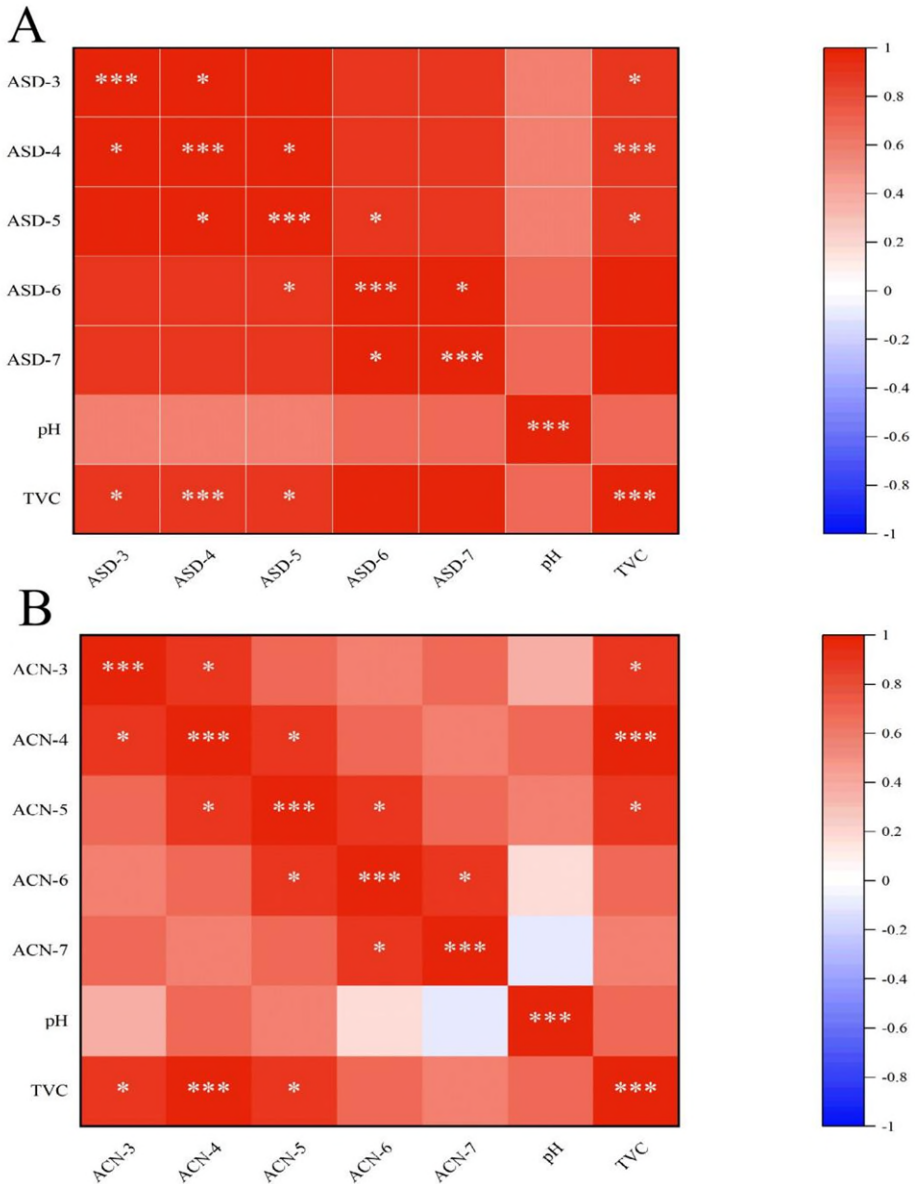


Fig. 7. Pearson correlation heatmaps between the total color difference ΔE of hydrogel beads and shrimp freshness indicators during storage at 4 °C.

(A) ASD-loaded hydrogel beads prepared at initial pH 3–7.

(B) Native anthocyanin-loaded hydrogel beads prepared at initial pH 3–7.

ASD, anthocyanin sulfite derivative; ACN, native anthocyanin; TVC, total viable count. Color scale represents Pearson's correlation coefficient (r). Positive and negative correlations are shown in red and blue, respectively. * ($p < 0.05$); *** ($p < 0.001$).

4. Conclusion

This study prepared anthocyanin sulfite derivatives (ASD) through reversible bisulfite addition and immobilized them in pectin–alginate hydrogel beads, demonstrating their feasibility for

shrimp freshness monitoring. ASD showed markedly reduced visible absorption over the pH range of 2–7 and regained visible absorption near pH 8. The similar transition pH values obtained during forward and reverse titration confirmed the reversibility of this color response. After immobilization, the ΔE values of ASD-loaded hydrogel beads remained between 1.19 and 1.55 at pH 2–5 but increased to 9.30 at pH 8, indicating that the pectin–alginate hydrogel retained the pH-responsive behavior of ASD. Compared with native anthocyanin-loaded hydrogel beads, ASD-loaded beads showed an increase in the final ΔE from 4.20 to 5.83 during ammonia exposure, corresponding to an improvement of 38.8%. Meanwhile, the t_{95} decreased from 12.22 to 6.83 min, representing a 44.1% reduction in response time. During shrimp storage at 4 °C, when the TVC reached 5.01 lg(CFU/g) on day 4, the ΔE of ASD-loaded beads prepared at an initial pH of 4 reached 4.38, compared with 1.76 for the corresponding native anthocyanin-loaded beads. These results indicate that reversible bisulfite derivatization provided a low-color baseline, defined a distinct response in the neutral-to-alkaline pH range, and accelerated the response to ammonia, thereby providing an earlier and more distinguishable visual indication of shrimp freshness loss. This strategy provides a feasible approach for improving the response performance of natural pigment-based freshness indicators for intelligent food packaging.

Author contribution

Haomiao Liu: Methodology, Investigation, Formal analysis, Data curation, Visualization, Writing – original draft. Xin Li: Methodology, Investigation, Validation. Qinnan Liu: Investigation, Validation. Xin Jia: Conceptualization, Supervision, Funding acquisition, Writing – review & editing. Lijun Yin: Conceptualization, Supervision, Project administration, Funding acquisition, Writing – review & editing.

Declaration of competing interest

The authors declare that they have no known competing financial interests or personal relationships that could have appeared to influence the work reported in this paper.

Acknowledgements

This work was supported by National Key Research and Development Program of China (No.2024YFD2101302), Sichuan Science and Technology Program, the National Nature Science Foundation of China (No. 32272337&32572555), Natural Science Foundation of Sichuan Province (No.2025ZNSFSC0229), Inner Mongolia Central Guidance on Science and Technology Development Funds (2024ZY0051), and 2115 Talent Development Program of China Agricultural University.

Data Availability

The data supporting the findings of this study are available within the article and its Supplementary Information. Additional raw data are available from the corresponding author upon reasonable request.

References

Almasi, H., Forghani, S., Moradi, M., 2022. Recent advances on intelligent food freshness indicators; an update on natural colorants and methods of preparation. Food Packaging and Shelf Life 32, 100839. https://doi.org/10.1016/j.fpsl.2022.100839

Bao, Y., Cui, H., Tian, J., Ding, Y., Tian, Q., Zhang, W., Wang, M., Zang, Z., Sun, X., Li, D., Si, X., Li, B., 2022. Novel pH sensitivity and colorimetry-enhanced anthocyanin indicator films by chondroitin sulfate co-pigmentation for shrimp freshness monitoring. Food Control 131. https://doi.org/10.1016/j.foodcont.2021.108441

Berké, B., Chèze, C., Vercauteren, J., Deffieux, G., 1998. Bisulfite addition to anthocyanins:: Revisited structures of colourless adducts. Tetrahedron Lett. 39, 5771–5774. https://doi.org/10.1016/S0040-4039(98)01205-2

Brouillard, R., Elhagechahine, J., 1980. Chemistry of anthocyanin pigments .6. Kinetic and thermodynamic study of hydrogen sulfite addition to cyanin - formation of a highly stable meisenheimer-type adduct derived from a 2-phenylbenzopyrylium salt. J. Am. Chem. Soc. 102, 5375–5378. https://doi.org/10.1021/ja00536a043

Chan, S.Y., Choo, W.S., Young, D.J., Loh, X.J., 2017. Pectin as a rheology modifier: Origin, structure, commercial production and rheology. Carbohydrate Polymers 161, 118–139. https://doi.org/10.1016/j.carbpol.2016.12.033

Cui W., Yang X., Zhang Y., Yin L., Jia X., 2026. Tailoring pectin functionality through controlled methoxylation: Insights into physicochemical characteristics and Ca2+-induced gelation mechanisms. Food Hydrocolloids 174, 112379. https://doi.org/10.1016/j.foodhyd.2025.112379

Einhorn-Stoll, U., 2018. Pectin-water interactions in foods - from powder to gel. Food Hydrocolloids 78, 109–119. https://doi.org/10.1016/j.foodhyd.2017.05.029

Feitosa, B.F., Decker, B.L.A., de Brito, E.S., Marques, M.C., Rodrigues, S., Mariutti, L.R.B., 2025. Anthocyanins stability theory – evidence summary on the effects of microencapsulation. Food Bioprod. Process. 153, 77–86. https://doi.org/10.1016/j.fbp.2025.06.001

Jurd, L., 1964. Reactions Involved in Sulfite Bleaching of Anthocyanins. Journal of Food Science 29, 16–19. https://doi.org/10.1111/j.1365-2621.1964.tb01685.x

Kaewprachu, P., Jaisan, C., Rawdkuen, S., Osako, K., 2024. Colorimetric indicator films based on carboxymethyl cellulose and anthocyanins as a visual indicator for shrimp freshness tracking. Heliyon 10. https://doi.org/10.1016/j.heliyon.2024.e31527

Kim, H.-J., Roy, S., Rhim, J.-W., 2022. Gelatin/agar-based color-indicator film integrated with Clitoria ternatea flower anthocyanin and zinc oxide nanoparticles for monitoring freshness of shrimp. Food Hydrocolloids 124, 107294. https://doi.org/10.1016/j.foodhyd.2021.107294

Liu, D., Zhang, C., Pu, Y., Chen, S., Liu, L., Cui, Z., Zhong, Y., 2022. Recent Advances in pH-Responsive Freshness Indicators Using Natural Food Colorants to Monitor Food Freshness. Foods 11, 1884. https://doi.org/10.3390/foods11131884

Luo, X., Zaitoon, A., Lim, L., 2022. A review on colorimetric indicators for monitoring product freshness in intelligent food packaging: Indicator dyes, preparation methods, and applications. Comp Rev Food Sci Food Safe 21, 2489–2519. https://doi.org/10.1111/1541-4337.12942

Mercanti, N., Macaluso, M., Pieracci, Y., Flamini, G., Scappaticci, G., Marianelli, A., Zinnai, A., 2024. Towards sulphite-free winemaking: A new horizon of vinification and maturation. Foods 13, 1108. https://doi.org/10.3390/foods13071108

Mohammadalinejhad, S., Almonaitytė, A., Jensen, I.-J., Kurek, M., Lerfall, J., 2023. Alginate microbeads incorporated with anthocyanins from purple corn (Zea mays L.) using electrostatic extrusion: Microencapsulation optimization, characterization, and stability studies. International Journal of Biological Macromolecules 246, 125684. https://doi.org/10.1016/j.ijbiomac.2023.125684

Mohammadalinejhad, S., Jensen, I.-J., Kurek, M., Lerfall, J., 2024. Novel colorimetric indicators based on alginate hydrogel beads containing anthocyanin for visual freshness monitoring of shrimp and minced chicken. LWT 199, 116127. https://doi.org/10.1016/j.lwt.2024.116127

Mohseni-Shahri, F.S., Moeinpour, F., 2023. Development of a pH-sensing indicator for shrimp freshness monitoring: Curcumin and anthocyanin-loaded gelatin films. Food Science & Nutrition 11, 3898–3910. https://doi.org/10.1002/fsn3.3375

Noël, M., Carballido, L., Bou-Maroun, E., Karbowiak, T., 2026. Sulfites chemistry in wines: From reference quantification methods to more sustainable innovative approaches. Compr. Rev. Food Sci. Food Saf. 25, e70396. https://doi.org/10.1111/1541-4337.70396

Reichembach, L.H., de Oliveira Petkowicz, C.L., 2021. Pectins from alternative sources and uses beyond sweets and jellies: An overview. Food Hydrocolloids 118. https://doi.org/10.1016/j.foodhyd.2021.106824

Timberlake, C., Bridle, P., 1967. Flavylium salts anthocyanidins and anthocyanins .2. Reactions with sulphur dioxide. J. Sci. Food Agric. 18, 479-,. https://doi.org/10.1002/jsfa.2740181009

Viscusi, G., Gorrasi, G., 2024. Blueberry extract loaded into rice milk/alginate-based hydrogels as pH-sensitive systems to monitor the freshness of minced chicken. Int. J. Biol. Macromol. 282, 137210. https://doi.org/10.1016/j.ijbiomac.2024.137210

Yan, F., Zhong, J., Chen, J., Liu, W., Chen, X., 2022. Application of alginate oligosaccharide produced by enzymatic hydrolysis in the preservation of prawns. Food Biosci. 49. https://doi.org/10.1016/j.fbio.2022.101897

Zheng, L., Liu, L., Yu, J., Shao, P., 2022. Novel trends and applications of natural pH-responsive indicator film in food packaging for improved quality monitoring. Food Control 134, 108769. https://doi.org/10.1016/j.foodcont.2021.108769

Supplementary Files

This is a list of supplementary files associated with this preprint. Click to download.

- SupplementaryInformation.docx